ASSESSMENT SYSTEM OF GIS-OBJECTS USING MULTI-TEMPORAL IMAGERY FOR NEAR-REALTIME DISASTER MANAGEMENT

D. Frey*, M. Butenuth

Remote Sensing Technology, Technische Universität München,
Arcisstr. 21, 80333 München, Germany – daniel.frey@bv.tum.de, matthias.butenuth@bv.tum.de

KEY WORDS: Change Detection, Classification, Integration, Multitemporal, Multisensor, Fusion, Disaster

ABSTRACT:

In this paper, a damage assessment system of GIS-objects such as roads and buildings after natural disasters is presented. The main contribution is the integration and exploitation of multi-temporal imagery leading to a more robust assessment of infrastructural objects. In addition, the chronological development of the assessed objects is investigated. The multivariate alteration detection method is used to detect changes between different time points in conjunction with the classification of different changes realized via Gaussian mixture models. Further accessorily introduced information are derived from GIS, in particular DEM belief functions. The strategy of the proposed approach is the combination of the computed probabilities using individual appropriate methods. The goal of the system is the assignment of GIS-objects into different damage assessment categories as intact or not intact/destroyed using the fused information from multi-temporal multi-sensorial data. The system is tested at a test scenario assessing roads concerning their trafficability. The results show the improvement of the damage assessment system after the integration of multi-temporal information.

1. INTRODUCTION

In this paper, an assessment system of GIS-objects is presented using multi-sensorial and multi-temporal imagery after natural disasters. The focus of this article is the multi-temporal component, because the integration of imagery from different time points into an assessment system has several advantages: Firstly, multi-temporal images provide the opportunity to monitor natural disaster chronologically during a period of time, not only at a specific time point. Secondly, the assessment of the GIS-objects at the time point t_2 can be improved using the results from time point t_1.

Another focus of this article is the automatic information retrieval from imagery being relevant for rescue teams after natural disasters. Information on the status of the infrastructure after disasters is essential to guarantee an effective and fast disaster management. Therefore, the emphasis of this article is the development of automated methods assessing infrastructural objects such as roads concerning their functionality.

The precondition ensuring an effective disaster management is the near-realtime supply of information, because time is the crucial parameter. Therefore, great efforts have been made in order to speed up the workflow from satellite tracking and data acquisition to the point of map generation (Voigt et al., 2007). The whole workflow can generally be passed within 24 hours. Data analysis consisting of information extraction, damage assessment, thematic analysis and change detection plays a decisive role in the processing chain of the workflow (Bamler et al., 2005). Up to now a lot of data analysis tasks are done manually which is very time consuming. Therefore, automation is required to substitute the manual interpretation. The difficulty is the development of methods minimizing wrong decisions to avoid fatal consequences in emergency actions. Possibilities to achieve a low error rate are semi-automated approaches.

A given fact is the variability of available imagery and GIS data in case of emergency. For this reason, a basic characteristic of the presented system is the handling of different input data sources.

---
* Corresponding author.

In this article, a modular system is presented which is able to deal with varying data sources and provides the embedding of all available information.

In Section 2. existing up-to-date damage assessment systems are presented and categorized in *area-* and *object-based systems*. In addition, data fusion techniques with regard to disaster management are discussed. Hereupon, the basics of Gaussian mixture model and a the change detection methods are introduced since these methods are key elements of the assessment system, which is described in Section 3. In Section 4. the general system is applied to a test scenario, the shown results are evaluated concerning their quality measure. Finally, further investigations and future work is pointed out.

2. STATE OF THE ART AND BASICS

2.1 Damage Assessment Systems

In case of natural disaster it is reasonable to differentiate between *object-based* and *area-based* damage assessment systems. The focus of *object-based systems* is the assessment of infrastructural objects such as roads or buildings concerning their functionality. In recent years several systems have been developed estimating the extent and type of destruction on various buildings. The damage assessment was realized using different kind of sensors such as LIDAR (Rehor et al., 2008) or satellite images (Chesnel et al., 2007). But there is a lack of methods assessing transportation lifelines after natural disasters (Morain and Kraft, 2003). In (Frey and Butenuth, 2009) a near-realtime assessment system of roads using GIS-objects and multi-sensorial data is presented. The road objects are classified into different states and are visualized using the ample paradigm proposed by Förstner (Förstner, 1996). In this article, the system is extended by the multi-temporal component using change detection methods.

On the other hand *area-based systems* focus on the affected regions. Typical examples are the generation of flood masks derived from different sensors. Besides optical imagery, particularly radar images are suitable for the extraction of inundated areas. Martinis (Martinis et al., 2009) uses a split-based automatic

thresholding method to detect flooded areas from TerraSAR-X data in near real-time.

2.2 Data fusion

In general, the performance of the damage assessment system can be improved by adding additional imagery and data sources. The additional benefit depends on the way of how the data is combined. Pohl (Pohl and Van Genderen, 1998) differentiate between three different levels of image fusion: pixel level, feature level and decision level. The combination of different data sources, e.g. vector and image data, was discussed in several other contributions, e.g. (Butenuth et al., 2007). Particularly, the integration of GIS information combined with imagery improves the results and simplifies the decision makings enormously (Brivio et al., 2002). Wang (Wang et al., 2002) presents a method for mapping flood extend combining optical imagery and DEM. In the approach, for each data source an individual flood mask is generated. The final flood mask consists of the set union of the individual masks. Considering the DEM as an image this approach belongs to the decision level image fusion as defined in (Pohl and Van Genderen, 1998). The presented approach in this article combines imagery and DEM, too, to detect flooded areas. In contrast to the discussed approaches, the aim is the combination based on probabilities derived from the input data.

2.3 Change Detection: Multivariate Alteration Detection (MAD)

Change detection algorithms are widely used investigating the extent and damage of natural disasters. A comprehensive review about change detection methods is given in Lu (Lu et al., 2004). However, many methods are restricted to specific sensors characteristics. The efficient response in case of natural disaster requires a change detection method which is able to deal with various sensors containing a different number of channels. Furthermore, the influence of changing atmospheric conditions should be minimized. The multivariate alteration detection method (MAD) is invariant to linear transformations which implies the insensitivity to linear atmospheric conditions or sensor calibrations at two different times. In addition, the handling of different numbers of channels is given (Nielsen et al., 1998).

The MAD transformation is based on the canonical correlation analysis (CCA). The CCA investigates the intercorrelation between two sets of variables unlike the principal component analysis, which identifies patterns of relationship within one set of data. Let $\mathbf{F} = \{F_1, F_2, ..., F_n\}$ and $\mathbf{G} = \{G_1, G_2, ..., G_m\}$ being two images with n or m channels ($n \leq m$). A linear combination of the intensities for all channels leads to the transformed images U and V:

$$\begin{aligned} U &= \vec{a}\,\mathbf{F} &= a_1 F_1 + a_2 F_2 + \ldots + a_n F_n \\ V &= \vec{b}\,\mathbf{G} &= b_1 G_1 + b_2 G_2 + \ldots + b_m G_m. \end{aligned} \quad (1)$$

The goal of the transformation is to choose the linear coefficient $\vec{a}$ and $\vec{b}$ minimizing the correlation between U and V. This leads to the result that the difference image between the transformed images U and V will have maximum variance. Due to the fact that multiples of U and V would have the same correlation a reasonable constraint $var(U) = 1$ and $var(V) = 1$ is chosen:

$$\begin{aligned} var(U - V) &= var(U) + var(V) - 2cov(U, V) \\ &= 2(1 - cov(U, V)). \end{aligned} \quad (2)$$

Using CCA, the linear coefficients $\vec{a}$ and $\vec{b}$ are determined and the MAD variates M_i can be calculated (Nielsen et al., 1998):

$$M_i = U_i - V_i \quad \text{for} \ i = 1 \ldots n. \quad (3)$$

An extension to the MAD transformation is the iterative reweighted MAD (IRMAD) method. Similar to boosting methods in data mining, an iteration schema focuses on observations whose change status is uncertain (Nielsen, 2007). Since the MAD or IRMAD variates can only being interpreted in a statistical manner there is a need to assign semantic meaning to the MAD variates. In Canty (Canty and Nielsen, 2006) an unsupervised classification method is proposed based on the MAD variates to cluster pixel in no-change and one or more change categories.

2.4 Combination of Probability Functions: Gaussian Mixture Model (GMM)

Since the radiometric characteristics of infrastructural objects of the same type could vary strongly, single probability functions are not able to describe the complex scenes sufficiently. Therefore, mixture models which combines single functions to a more complex probability function are used. The resulting probability function $p(\mathbf{y}|\theta_j)$ is simply a weighted sum of the initial functions $p(\mathbf{y}|\theta_j)$:

$$p(\mathbf{y}|\theta) = \sum_{j=1}^{k} \alpha_j p(\mathbf{y}|\theta_j). \quad (4)$$

Each θ_j describes the set of parameters defining the jth component, $\alpha_1 \ldots \alpha_j$ are the weights called mixing probabilities and $\mathbf{y} = [y_1 \ldots y_d]^{\mathrm{T}}$ represent one particular outcome of a d-dimensional random variable $\mathbf{Y} = [Y_1 \ldots Y_d]^{\mathrm{T}}$. If $\mathbf{Y}$ is normal distributed, Gaussian are typically used. The mixing probabilities have to fulfill following equations:

$$\alpha_j \geq 0, \quad j = 1 \ldots k, \quad \text{and} \quad \sum_{j=1}^{k} \alpha_j = 1. \quad (5)$$

The expectation maximization (EM) algorithm is used to determine α_j and θ_j. A detailed description of mixture models can be found in McLachlan (McLachlan and Peel, 2000). The minimum message length criterion (MML) is one possibility to find the number of centers j and is used in our system (Figueiredo and Jain, 2002).

3. ASSESSMENT SYSTEM

In this Section, the general assessment system is presented using multi-sensorial multi-temporal imagery and further available data. The goal is the assessment of GIS-objects categorizing them into different states.

3.1 System

The design of the system has a modular and very flexible structure to cope with varying raw data being available in emergency cases (cf. Fig. 1). Nevertheless, there are some prerequisites to apply the system. The GIS-objects which should be assessed concerning their functionality must be given. It is conceivable to extract the GIS-objects using imagery before the natural disaster takes place or, alternatively, from a GIS. However, in view of the performance of automatic extraction methods, objects from a given GIS-database with a guaranteed quality are better suited. The result of the assessed GIS-objects depends strongly on the
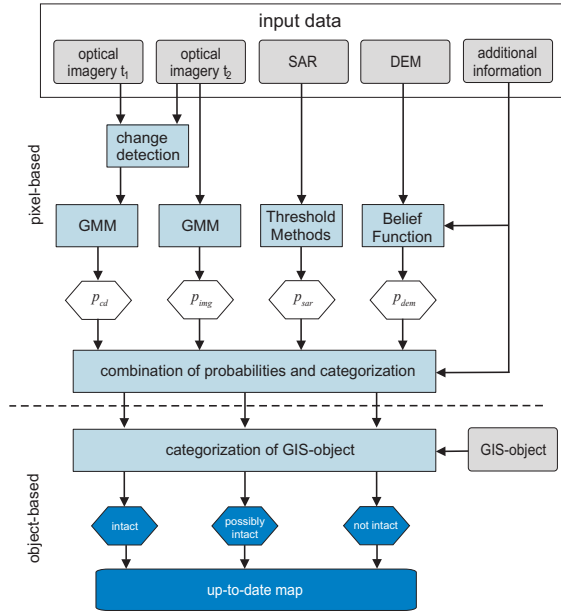
In: Wagner W., Székely, B. (eds.): ISPRS TC VII Symposium – 100 Years ISPRS, Vienna, Austria, July 5–7, 2010, IAPRS, Vol. XXXVIII, Part 7A

Contents   Author Index   Keyword Index

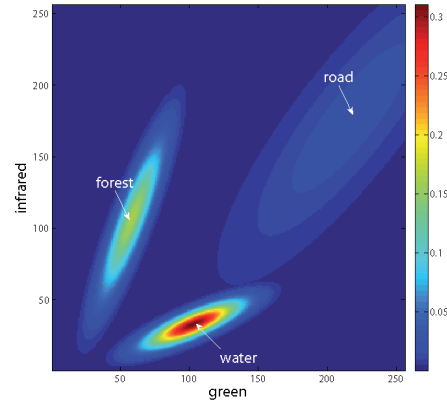Figure 1: General damage assessment system.

Figure 2: Two-dimensional probability density functions of the classes forest, water and a combined class road. Exemplarily visualized via the infrared and green channel.
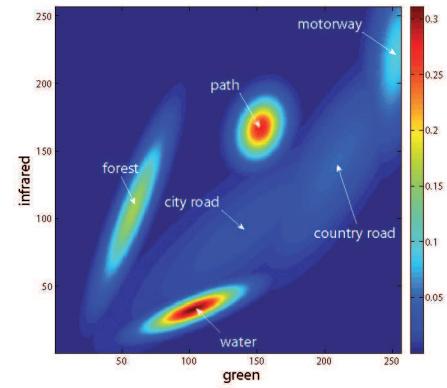

Figure 3: Two-dimensional probability density functions of the classes forest, water and separated road-classes (city road, country road, path and motorway). Exemplarily visualized via the infrared and green channel.

available input information. Besides the imagery, DEM and further GIS-information can be embedded into the system. Here, this data is called input data.

For multispectral imagery Gaussian mixture models are applied. Belief functions are introduced to derive probabilities from GIS-information. If multi-temporal imagery are available change detection methods such as the MAD algorithm are used to derive probabilities. The combination of the different input data is carried out in the probability level. All the individual methods and the combination of the probabilities are realized at pixel level. In contrast, the subsequent assignment of GIS-objects to the categories *intact*, *possibly intact* or not *intact/destroyed* using a maximum likelihood estimation is object-based (cf. Fig. 1).

3.2 Methods and Combination of Probabilities

For each input data individual methods have to be applied to derive individual probabilities if the infrastructural objects are intact or not (cf. Fig. 1). Given multispectral imagery as input data a multispectral classification is carried out. The infrastructural objects are classified to different classes relating to the categories *intact*, *possibly intact* and not *intact/destroyed*. Since a lot of classes like roads have no consistent radiometric characteristic as shown in Figure 2 and Figure 3, GMM are used to deal with the different subgroups of the classes. The resulting probabilities from the mixture model p_{img} are combined with probabilities from further input data (cf. Fig. 1).

The availability of images at different time points enables the usage of change detection methods exploiting additional assessment criteria. The IRMAD algorithm enables the detection of changes caused by natural disasters. The resulting IRMAD-variates are classified using a supervised multispectral classification. For the different change-classes, i.e. 'intact ⇒ destroyed' probability functions are generated. These probabilities p_{mad} are embedded into the assessment system. In Figure 4(c) three IRMAD variates are shown as an RGB-color image obtained from IKONOS-images at time t_1 (cf. Fig. 4(a)) and time t_2 (cf. Fig. 4(b)). In this example of a flood event the changed areas from flooded to not flooded are illustrated in pink, the gray color stands for no change (cf. Fig. 4(c)).
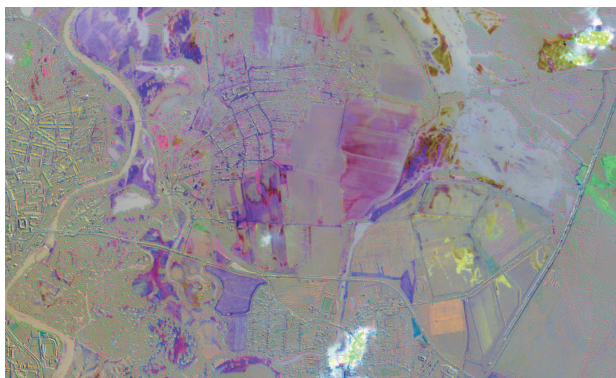
Additional GIS-information such as DEM is often available having the opportunity to enhance the assessment system. Since the combination of the input data is based on the probability level, also from the GIS-information probabilities have to be derived. Belief functions can be generated depending on the GIS-information. In Figure 5 an example is shown, which depicts the probability that an object is flooded depending on the altitude. The combination of the probabilities derived from the different input data is defined as following (cf. Fig. 1):

$$p_{s_1} = p_{s_1,img} \otimes p_{s_1,gis} \otimes \ldots \otimes p_{s_1,mad}$$
$$p_{s_2} = p_{s_2,img} \otimes p_{s_2,gis} \otimes \ldots \otimes p_{s_2,mad}$$
$$\vdots \qquad (6)$$
$$p_{s_i} = p_{s_i,img} \otimes p_{s_i,gis} \otimes \ldots \otimes p_{s_i,mad}.$$

The probabilities p_{s_i} are the combined probabilities of one status s_i. In the easiest case the set of states could be *intact* or *not intact*. But it is also possible to think of different kinds of destruction states. In addition, weights are introduced since the information content of the different input data varies:

$$p_{s_i} = w_1 p_{s_i,img} \otimes w_2 p_{s_i,gis} \otimes \ldots \otimes w_d p_{s_i,mad}. \qquad (7)$$

The number of input data is denoted as d. Finally, the object is categorized to the state s_i with the largest probability.

In: Wagner W., Székely, B. (eds.): ISPRS TC VII Symposium – 100 Years ISPRS, Vienna, Austria, July 5–7, 2010, IAPRS, Vol. XXXVIII, Part 7A

Contents   Author Index   Keyword Index

(a) IKONOS-scene of flooded area at time t_1

(b) IKONOS-scene of flooded area at time t_2

(c) Three MAD-variates depicted as an RGB-color image

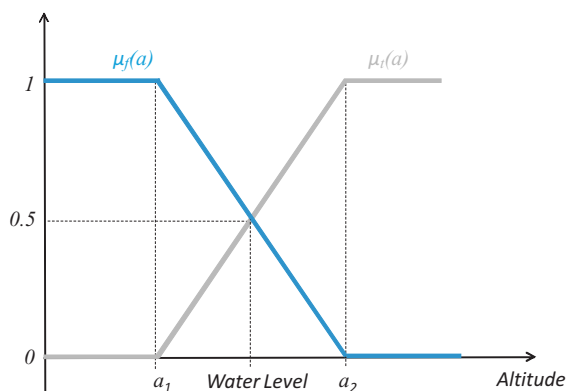Figure 4: Change detection using MAD-algorithm.

Figure 5: Belief functions depending on altitude: area is flooded (blue), area is not flooded (gray).

4. RESULTS AND DISCUSSION

The presented damage assessment system is applied to a specific flood scenario. In real case scenarios the availability of input data is the crucial factor. The derivation of the probabilities given in Equation 6 is not always possible depending on the available data. On the other side often additional information exist which are useful to generate additional rules. In real applications the combination of probabilities is embedded into a rule-based framework which can differ from case to case.

4.1 Test Scenario

Test scenario is the flooding of the river Elbe (Germany) in the year 2002. The available input data for the damage assessment system consists of two IKONOS-scenes (cf. Fig. 4(a) and 4(b)) acquired at the 21th and 26th of August, and a DEM. The peak of the water level was measured at the 19th of August. The scene at the time t_1 shows almost the maximum inundated area. In the second scene at time t_2 the flooding receded strongly and only a small area is covered by water (cf. Fig. 4(b), top right). In addition to the images, a DEM is available with a 10m x 10m grid with an geometric accuracy of +/- 1m. In this test scenario road objects given from a GIS-database are assessed concerning their trafficability.

4.2 Workflow of Rule-based Classification

A detailed workflow of the rule-based assessment system is depicted in Figure 6, the input data are illustrated by gray parallelograms. Below these parallelograms the derived probabilities from the input data are attached in gray rectangles. The combination of the probabilities is realized in the blue boxes. The goal in this scenario is the assessment of road segments concerning the trafficability at time t_2. In addition to the imagery and the DEM described in Section 4.1, the assessed road segments at the time t_1 are given. They are obtained by means of the described assessment system using very strict parameters. Alternatively, also a manual generated reference at time t_1 could be used. The assessed road segments at time t_1 and additional information as the water level lead to the rule-based framework built on the combination of the probabilities. The probability p_{img} derived from the imagery is partitioned into three different probabilities belonging to a specific class: water p_{water}, road p_{road}, forest p_{forest}. As shown in Figure 3 the class road is subdivided into subclasses of roads using GMM. Using a maximum likelihood estimation followed by a threshold operation the segment is categorized into the three states *trafficable*, *possibly flooded* and *flooded*.

4.3 Evaluation

The obtained results are compared to a manually generated reference. The information for the generation of the reference is only the image at time t_2. Therefore, it is not a comparison with the real ground truth, but it is the comparison of the automatic approach with the manually interpretation of an human operator. The reference is also categorized into three different classes *trafficable*, *possibly flooded* and *flooded*. Since the categorization of the automatic system consists of the same states the following four different assignment criteria are determined: 'correct assignment', 'manual control necessary', 'possibly correct assignment' and 'wrong assignment'. The category 'correct assignment' means that the manually generated reference is identical with the result of the automatic system. In the case of 'manual control necessary' the automatic approach leads to the state *possibly flooded* whereas the manual classification assigns the line segments to *flooded* or *trafficable*. The other way around

In: Wagner W., Székely, B. (eds.): ISPRS TC VII Symposium – 100 Years ISPRS, Vienna, Austria, July 5–7, 2010, IAPRS, Vol. XXXVIII, Part 7A

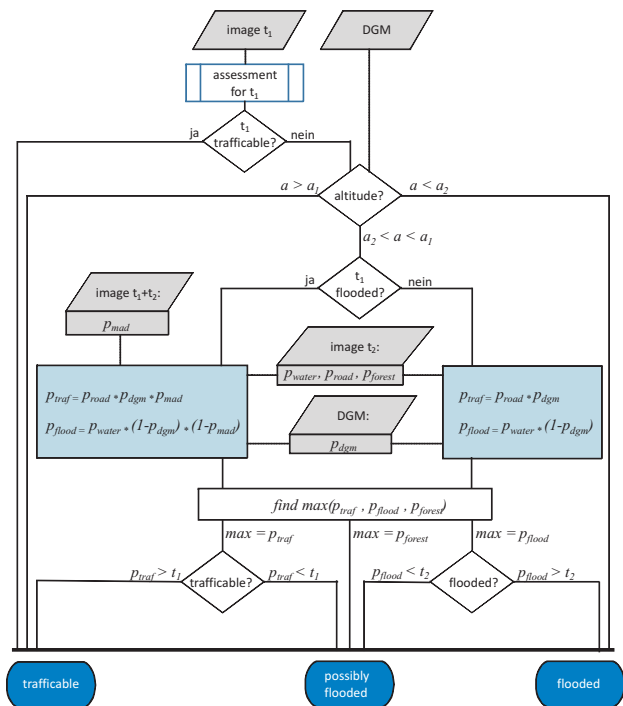Contents   Author Index   Keyword Index

Figure 6: Workflow of Rule-based Classification.

denotes the expression 'possibly correct assignment'. 'wrong assignment' means that one result categorize the segment to *flooded* and the other to *trafficable*. The enhancement of the automatic system by the combined interpretation is shown in Table 7.

	t_2	t_2, DEM	$t_{1,2}, DEM$	$t_{1,2,c}, DEM$
correct	68.40	68.45	69.60	87.14
manual	27.88	27.77	27.48	10.96
possibly	2.64	2.72	2.52	1.79
wrong	1.08	1.06	0.40	0.11

Table 7: Evaluation (percentage shares)

The first column in Table 7 represents the result using only the image t_2 without any further information. The result with about 1% of 'wrong assignements' and about 68% 'correct assignment' is almost identical if an additional DEM as input data is used (cf. Table 7: t_2, DEM). The reason for the lack of improvement could be ascribed to the bad accuracy of the used DEM. The influence of the height information is discussed in (Frey and Butenuth, 2009). The evaluated road segments are depicted in Figure 8(a). Green road segments correspond to 'correct assignment', yellow to 'manual control necessary', cyan to 'possibly correct assignment' and red or blue belongs to 'wrong assignment'. If the systems assigns a road segment to the category *trafficable* but the referencce is *flooded* the road segment is colored in red. Blue road segments are assigned to *flooded* by the system and *trafficable* by the reference.

In Figure 8(b) the result of the third column from Table 7 is visualized which includes the additional scene at time point t_1 as input data. The additional scene and the resultant calculated probability p_{mad} derived from the described MAD method leads to an improvements of the results. Several red road segments disappear whereas the 'correct assignments', the assignments to 'manual control necessary' and the 'possibly correct assignments' remains almost constant.

In Figure 8(c) the results exploiting an additional manually generated reference from scene t_1 are plotted. The numerical eval-

(a) Detail of evaluation using image t_2 and DEM

(b) Detail of evaluation using image t_2, image t_1 and DEM

(c) Detail of evaluation using image t_2, image t_1 with correctly assessed roads and DEM

Figure 8: Evaluation of assessment system: green='correct assignment', yellow='manual control necessary', cyan='possibly correct assignment', red='wrong assignment'[system = *trafficable*, reference = *flooded*], dark blue = 'wrong assignment' [system = *flooded*, reference = *trafficable*].

uation is presented in the forth column of Table 7 ($t_{1,2,c,DEM}$). The results are by far better then the previous obtained results. The 'correct assignments' arise from 69% to 87% and the 'wrong assignments' decrease from 0.4% to 0.1%. But it is important to point out, that a correct reference at the time point t_1 has to be generated. Nevertheless, it has no influence of the fact that the system is near-realtime since the time consuming generation of the reference can be done before.

4.4 Result after Data Fusion

The final obtained result using the described damage assessment system is depicted in Figure 9. All road segments are divided

In: Wagner W., Székely, B. (eds.): ISPRS TC VII Symposium – 100 Years ISPRS, Vienna, Austria, July 5–7, 2010, IAPRS, Vol. XXXVIII, Part 7A

Contents   Author Index   Keyword Index

into four different categories. Besides the already mentioned categories *trafficable* (green), *possibly flooded* (yellow) and *flooded* (red) an additional category *flooded to trafficable* (blue) is introduced by means of the change detection algorithm. This additional category is very useful for rescue teams since it shows the areas which are again trafficable after flooding.
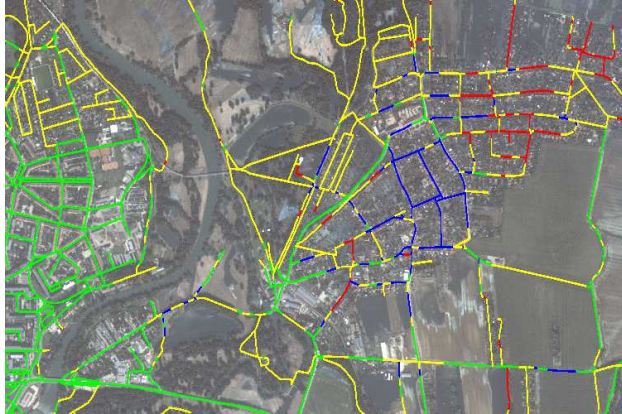

Figure 9: Detail of result of damage assessment system using all available input data: image t_1, imaget_2, DEM and manual generated reference at time t_1. (green = *trafficable*, yellow = *possibly flooded*, red = *flooded*, dark blue = *flooded $\Rightarrow$ trafficable*).

5. CONCLUSIONS

In this article, the general framework of a damage assessment system and the benefit of the included data fusion is shown. The improvement of the results by adding additional available data is demonstrated in the test scenario. The integration of multitemporal imagery leads to an enhancement of the damage assessment system concerning the correctness of the assessed objects and concerning the additional temporal information which can provide the rescue teams in emergency actions. Combining this basis with rule-based approaches which are strongly dependent on the natural disasters and available input data the overall system leads to useful results with a very little rate of 'wrong assignments'.

In future work, the generic system will be tested at more test scenarios with different sensors. In particular, the combination of optical images and radar images should be investigated in more detail. In addition, the influence of the DEM accuracy has to be investigated in future work. Besides the radiometric exploitation of the optical imagery also the geometric features should be introduced as an additional evidence of destructions. A distinction between different regions of global context should improve the results as well. Depending on the global context the required parameter can be chosen. The automatic setting of the parameters in the system is currently not included in this paper. Further investigations have to be done to learn suitable parameters automatically depending on the available data.

REFERENCES

Bamler, R., Reinartz, P., Riedlinger, T. and Schroeder, M., 2005. Moderne Raumfahrttechniken für Prävention bei Naturkatastrophen und das Krisenmanagement.

Brivio, P., Colombo, R., Maggi, M. and Tomasoni, R., 2002. Integration of remote sensing data and GIS for accurate mapping of flooded areas. International Journal of Remote Sensing 23(3), pp. 429–441.

Butenuth, M., Gösseln, G., Tiedge, M., Heipke, C., Lipeck, U. and Sester, M., 2007. Integration of heterogeneous geospatial data in a federated database. ISPRS Journal of Photogrammetry and Remote Sensing 62(5), pp. 328–346.

Canty, M. and Nielsen, A., 2006. Visualization and unsupervised classification of changes in multispectral satellite imagery. International Journal of Remote Sensing 27(18), pp. 3961–3975.

Chesnel, A.-L., Binet, R. and Wald, L., 2007. Quantitative assessment of building damage in urban area using very high resolution images. In: Urban Remote Sensing Joint Event, 2007, pp. 1–5.

Figueiredo, M. and Jain, A., 2002. Unsupervised learning of finite mixture models. IEEE Transactions on Pattern Analysis and Machine Intelligence 24(3), pp. 381–396.

Frey, D. and Butenuth, M., 2009. Classification system of GIS-objects using multi-sensorial imagery for near-realtime disaster management. In: International Archives of Photogrammetry, Remote Sensing and Spatial Information Sciences, Vol. XXXVIII(3/W4), pp. 103–108.

Förstner, W., 1996. Pros and cons against performance characterization of vision algorithms. In: Proceedings of ECCV Workshop on Performance Characteristics of Vision Algorithms, Cambridge, UK, April, pp. 215–218.

Lu, D., Mausel, P., Brondizio, E. and Moran, E., 2004. Change detection techniques. International Journal of Remote Sensing 25(12), pp. 2365–2401.

Martinis, S., Twele, A. and Voigt, S., 2009. Towards operational near real-time flood detection using a split-based automatic thresholding procedure on high resolution TerraSAR-X data. Natural Hazards and Earth System Science 9(2), pp. 303–314.

McLachlan, G. and Peel, D., 2000. Finite mixture models. Wiley-Interscience.

Morain, S. and Kraft, W., 2003. Transportation lifelines and hazards: Overview of remote sensing products and results. In: Proceedings of Remote Sensing for Transportation 29, pp. 39 – 46.

Nielsen, A., 2007. The regularized iteratively reweighted MAD method for change detection in multi- and hyperspectral data. IEEE Transactions on Image Processing 16(2), pp. 463–478.

Nielsen, A., Conradsen, K. and Simpson, J., 1998. Multivariate alteration detection (MAD) and MAF postprocessing in multispectral, bitemporal image data: New approaches to change detection studies. Remote Sensing of Environment 64(1), pp. 1–19.

Pohl, C. and Van Genderen, J., 1998. Multisensor image fusion in remote sensing: concepts, methods and applications. International Journal of Remote Sensing 19, pp. 823–854.

Rehor, M., Bähr, H., Tarsha-Kurdi, F., Landes, T. and Grussenmeyer, P., 2008. Contribution of two plane detection algorithms to recognition of intact and damaged buildings in lidar data. The Photogrammetric Record 23(124), pp. 441–456.

Voigt, S., Kemper, T., Riedlinger, T., Kiefl, R., Scholte, K. and Mehl, H., 2007. Satellite image analysis for disaster and crisis-management support. IEEE Transactions on Geoscience and Remote Sensing 45(6), pp. 1520–1528.

Wang, Y., Colby, J. and Mulcahy, K., 2002. An efficient method for mapping flood extent in a coastal floodplain using landsat tm and dem data. International Journal of Remote Sensing 23(18), pp. 3681–3696.